Journal of Microbiology, Immunology and Infection 56 (2023) 951–960

Available online at www.sciencedirect.com

ScienceDirect

journal homepage: www.e-jmii.com

Original Article

Inhalable chitosan-based hydrogel as a mucosal adjuvant for hydroxychloroquine in the treatment for SARS-CoV-2 infection in a hamster model

Donna Shu-Han Lin [a], Shian Chiuan Tzeng [b], Tai-Lung Cha [c], Chin-Mao Hung [c], Wen-Chin Lin [c,d], Chuen-Mi Yang [c], Hsuan-Ying Lu [c], Jia-Yu Chang [c], Shu-Wei Huang [e,*]

[a] *Division of Cardiology, Department of Internal Medicine, Shin Kong Wu Ho-Su Memorial Hospital, Taipei, Taiwan*
[b] *Department of Materials Science and Engineering, National Taiwan University of Science and Technology, Taipei, Taiwan*
[c] *Institute of Preventive Medicine, National Defense Medical Center, Taipei, Taiwan*
[d] *Department of Pathology and Graduate Institute of Pathology and Parasitology, Tri-Service General Hospital, National Defense Medical Center, Taipei, Taiwan*
[e] *Department of Orthopedics, Wan Fang Hospital, Taipei Medical University, Taipei, Taiwan*

Received 2 November 2022; received in revised form 20 April 2023; accepted 4 August 2023
Available online 15 August 2023

KEYWORDS
COVID-19;
SARS-CoV-2;
Chitosan oligosaccharide;
Hydroxychloroquine;
Drug inhalation

Abstract *Background:* Effective therapy for COVID-19 remains limited. Hydroxychloroquine (HCQ) has been considered, but safety and efficacy concerns remain. Chitosan exhibits antiviral and immunomodulatory effects, yet how the combination of HCQ and chitosan performs in treating COVID-19 is unknown.
Methods: Male Syrian hamsters were inoculated intranasally with standardized stocks of the SARS-CoV-2 virus. Hamsters were allocated to saline (PBS), chitosan oligosaccharide (COS), HCQ, or COS + HCQ groups and received corresponding drugs. On days 1, 7, and 14 post-infection, two animals from each group were euthanized for sample collection. Viral loads were measured in lung homogenates. Biochemistry markers, cytokines, and immunoglobulins were analyzed from hamster sera. HCQ concentrations were compared between the blood, bronchoalveolar lavage, and lung tissues. All groups underwent histopathology exams of the lungs. Additional hamsters were treated with the same drugs to assess for toxicities to the heart and liver.

* Corresponding author. No. 111, Sec. 3, Xinglong Rd., Wenshan Dist., Taipei City 116, Taiwan.
E-mail addresses: judyya1022@gmail.com, 111022@w.tmu.edu.tw (S.-W. Huang).

https://doi.org/10.1016/j.jmii.2023.08.001

Results: Among all groups, viral loads in the COS + HCQ group were the lowest by day 8. The COS + HCQ group produced the highest interleukin (IL)-6 levels on day 4, and the highest IL-10, IgA and IgG levels on day 8. HCQ concentrations were higher in the COS + HCQ group's lungs than the HCQ group, despite having received half the dose of HCQ. Histopathology demonstrated earlier inflammation resolution and swifter viral clearance in the COS + HCQ group. There was no evidence of cardiac or hepatic injury in hamsters that received HCQ.
Conclusion: In hamsters infected with the SARS-CoV-2 virus, the combination of intranasal COS and HCQ was associated with increased HCQ absorption in the lungs, more effective immune responses, without increasing the risk of hepatic or cardiac injuries.

Introduction

Since 2019, the severe acute respiratory syndrome Coronavirus-2 (SARS-CoV-2) has infected over 575 million individuals and led to more than six million deaths worldwide.[1] The SARS-CoV-2 is characterized by low fatality but great infectivity and transmissibility.[2,3] Clinical manifestations of COVID-19 range from asymptomatic infection to severe multiorgan failure 2. In elderly patients and those with multiple comorbidities, SARS-CoV-2 infection lead to worsened prognosis.[4,5] The goals of COVID-19 treatment include shortening viral shedding, inhibition of transmission, attenuation of disease severity, and prevention of long-term complications.[6]

Currently, drugs approved by or received Emergency Use Authorizations from the Food and Drug Administration of the United States for treatment of COVID-19 are limited by their high costs and paucity of evidence in milder disease.[7] In light of the rapidly mutating and spreading virus, a cheaper yet effective treatment is needed. Hydroxychloroquine (HCQ) gained attention after in vitro studies demonstrated inhibition of the SARS-CoV-2 with a low half-maximal effective concentration.[8,9] Its low costs, high accessibility and relatively safe drug profile has led to great interest in HCQ.[10] However, higher than usual doses of HCQ are required to achieve antiviral effects, yet high systemic doses of HCQ may lead to systemic toxicities.[11–13] Studies on the treatment of COVID-19 have noted a trend in increased mortality associated with HCQ,[14,15] leading to concerns for its use.

SARS-CoV-2 invades its hosts via the respiratory system.[16] Inhaled antiviral therapy allows high drug doses to be dispensed directly at the site of infection while minimizing systemic side effects.[17] Besides aiming for higher local doses, adding an adjunct to enhance drug biocompatibility and sustainability may also help. Chitosan poses an attractive option for intranasal drug delivery due to its mucoadhesive properties, high stability and low toxicity.[18] We hypothesize that HCQ exhibits antiviral effects augmented by combined chitosan oligosaccharide (COS) when administered directly in the respiratory tract. In this proof-of-concept study, we investigated the efficacy and safety of a novel inhaled combination of COS + HCQ for the treatment of COVID-19 in a hamster model.

Methods and materials

Ethics statement

This study was approved by the IACUC of Institute of Preventive Medicine, National Defense Medical Center (IACUC AN-110-32). Hamster procedures were performed under intraperitoneal anesthesia.

Virus

According to institutional guidelines, all virus-related work was conducted in high-containment Biosafety Level 3 (BSL3) facilities of the Institute of Preventive Medicine, National Defense Medical Center. All potentially infectious substances were treated to inactivate viral particles before leaving the BSL-3 facility. The SARS-CoV-2 isolate was provided by the Taiwan Center for Disease Control (BetaCoV, GISAID accession number EPI_ISL_411,915 and NCBI accession number MT192759, Taiwan CDC) and amplified in Vero E6 cells.

Viral titers of the supernatant were measured using a standard 50% tissue culture infectious dose (TCID50) assay. Cells plaques were counted to evaluate the cytopathic effect of the SARS-CoV-2 isolate, with the TCID50 calculated through the Reed-Muench method.

Chemicals and agents

Deacetylated COS (MW $<$ 2000, CAS number 9012-76-4), HCQ sulfate (CAS number 747-36-4), and phosphate buffer saline (PBS) were purchased from Sigma—Aldrich Chemie GmbH (Steinheim, Germany). Zoletil 50 was purchased from Virbac (Carros, France) and xylazine from Bayer (Leverkusen, Germany). The COS was dispersed in PBS and gently stirred for 1 h at 37 °C to dissolve completely. HCQ

sulfate powder 0.65 mg/kg was mixed completely with 0.4% (w/w) COS solution.

Administration of drugs and viral challenge in hamsters

Eight-week-old male Syrian hamsters were purchased from the National Laboratory Animal Center (NARLabs, Taipei, Taiwan) and maintained in the BSL3 facility accredited by the Association for Assessment and Accreditation of Laboratory Animal Care International. Sample sizes were determined according to the maximum housing capacity of BSL3 facilities. The animals were weighed and randomly separated into five groups, with seven in each group at 20 °C, 55% humidity and 12:12 day/night cycles.

Animals were infected on day 0 with 50 μl of virus-containing media containing approximately 10^4 PFU given intranasally under anesthesia (Supplemental Fig. 1). Control hamsters were given the same volume of sterile PBS similarly. One hour after infection, the animals were treated intranasally with the designated drug for each group: the PBS group received PBS only, the COS group 0.4% (w/v) COS solution at a concentration of 25 mmol/L, the COS + HCQ group a mixture of HCQ sulfate 0.65 mg/kg with 0.4% (w/w) COS solution, and the HCQ group HCQ at 1.3 mg/kg. Subsequent doses of each drug were given once every two days.

Animals were weighed and examined on a daily basis. On days 1, 7 and 14, two animals from each group were randomly selected and humanely euthanized for sample collection. The experiment was repeated twice.

In addition to the aforementioned experiments, five groups of nine hamsters each were treated according to the same protocol but without inoculation of virus stock to assess for drug-related cardiac and hepatic toxicities. On days 1, 7 and 14, three animals from each group were randomly selected and euthanized for collection of the heart and liver.

Virological analysis

RT-qPCR determined viral loads from lung homogenates. To ensure nucleic acid stability, DNA/RNA shield (Zymo research, CA, USA) was added to the lung homogenates after homogenization. Nucleic acids were extracted with the LabTurbo AIO Viral DNA/RNA Extraction Kit (Taigen Bioscience Co., TPE, TW). RT-qPCR was performed using the TaqMan Fast Virus 1-Step Master Mix (Applied Biosystems, CA, USA) with primer-probe sets targeting the SARS-CoV-2 E gene.[19] Primer sequences are shown in Table 1. RNA extraction and RT-qPCR were performed using the LabTurbo AIO 48 SP-qPCR System (Taigen Bioscience Co., TPE, TW), an all-in-one automated device. In vitro transcribed RNA standards containing SARS-CoV-2-E gene sequences were synthesized by using the HiScribeTM T7 Quick High Yield RNA Synthesis Kit (New England Biolabs, MA, USA). Dilutions of RNA standards were quantified using the QIAcuity Digital PCR system (Qiagen, NRW, GER), in combination with the QIAcuity One-Step Viral RT-PCR Kit (Qiagen, NRW, GER) to calculate viral genomic copies with RT-qPCR.

Serum biochemistry analysis

Hamster blood were collected on day 4, 8 and 14 after infection and centrifuged at 1300×*g* for 10 min to obtain plasma. Data on serum aspartate aminotransferase (AST), alanine aminotransferase (ALT), and lactate dehydrogenase (LDH) were examined by using a serum chemistry analyzer (Cobas C111, Roche, Basel, Switzerland).

Cytokine and antibody expression analysis

Analysis of expression of hamster interleukin (IL)-6 (CUSABIO Technology LLC, Houston, USA), IL-10 (CUSABIO Technology LLC, HOU, USA), IL-1β (CUSABIO Technology LLC, Houston, USA), the immunoglobulin A (IgA, MyBioSource Inc., CA, USA) and immunoglobulin G (IgG, Abcam Inc., Camb, UK) were conducted by ELISA. Data were determined via microplate readers capable of measuring absorbance at 450 nm, with the correction wavelength set at 570 nm.

Quantification of hydroxychloroquine

HCQ was detected via electrospray-ionization time-of-flight mass spectrometry (ESI-TOF MS). Data were collected through a mass spectrometer (JMS-T100LP4G, JEOL Ltd., Tokyo, Japan) equipped with an ESI source, detecting positive and negative ions. Typical measurement conditions were as follows: needle voltage 2000 kV, orifice 1 voltage 30 V, ring lens voltage 10 V, spray temperature 250 °C. HCQ concentration was quantified in blood, homogenized lung tissue, and bronchoalveolar lavage fluid.

Blood samples were collected in serum separator tubes (BD Vacutainer, sNJ, USA) and centrifuged to collect the serum. Serum samples were diluted into 25 μL aliquots with 100 μL of 0.1% formic acid and 1 ml of acetonitrile, vortexed and incubated at −20 °C for 2 h. Serum samples were centrifuged for clarification of the supernatant and then taken to dryness in a concentrator. Finally, the serum was

Table 1 Primer Sequences for RT-qPCR of the SARS-CoV-2 E gene.

Assay	Target	Primer/ Probe	Sequence (5'→3')[3]	Optimal working concentration (μM)
E	Envelope protein gene	E_Sarbeco_F1	ACAGGTACGTTAATAGTTAATA-GCGT	0.4
		E_Sarbeco_R2	ATATTGCAGCAGTACGCACACA	0.4
		E_Sarbeco_P1	**FAM**-ACACTAGCCATCCTTACTGCGCTTCG-BBQ	0.2

resuspended in 100 μL of 50% methanol, centrifuged again and the supernatant was collected again.

The bronchoalveolar lavage fluid was obtained after the lungs were taken out and flushed back and forth ten times with 3 ml of PBS injected into the bronchi. The bronchoalveolar lavage fluid was centrifuged to obtain the supernatant. The lung tissue was homogenized using Dulbecco's Modified Eagle Medium (DMEM, Life Technologies, NY, USA) and centrifuged to separate the supernatant for analysis. Subsequent preparation of lung tissue and bronchoalveolar lavage fluid samples is similar to the preparation of serum samples.

The calibration standards were prepared by spiking 100 Ul of blank sample with proper standard solutions of HCQ sulfate and 20 uL of internal standard solution. The effective concentration in analyzed samples was between 50 and 1000 ng/ml. The standards and controls were extracted for each analysis with the same procedures detailed previously.

Pathology assessment by histology

Hamsters were sacrificed and the lungs, liver and heart were obtained. Organs were fixed and embedded in paraffin for staining. The lungs were examined with the periodic acid schiff's stain (PAS), immunohistochemical staining (IHC), hematoxylin and eosin stain (H&E stain) and scanning electron microscope (SEM). The heart and liver slides were stained with H&E stains.

Statistical analysis

All statistical analyses were performed using the GraphPad Prism 8 software (GraphPad, San Diego, CA, USA). Results are presented as means and 95% confidence intervals. Statistical differences between groups were analyzed using the Tukey's multiple comparisons test and considered statistically significant at p values < 0.05 ($^{*}p < 0.05$, $^{**}p < 0.01$, $^{***}p < 0.001$). Histopathology of all specimens were examined blindly.

Results

Physiologic parameters

After intranasal inoculation of the SARS-CoV-2 virus, the hamsters displayed lethargy, with ruffled fur and hunched backs. At day 3, body weight of all infected hamsters began to fall and was significantly lower than the control group. Body weight of infected hamsters continued to decline until day 6; after day 6, slowly increased until day 14 (Supplemental Fig. 2). There were no significant differences between each group regarding changes in body weight.

Viral loads

The cycle threshold (CT) value of SARS-CoV-2 E gene in the homogenized lung tissues increased in all hamster groups as time went by after infection (Fig. 1). On day 8, there seems to be a trend towards lower viral loads in the COS + HCQ group compared to other groups (Supplemental Fig. 3).

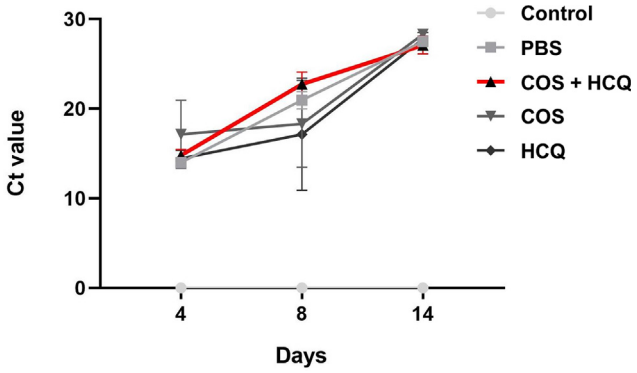

Figure 1. Viral loads in the lung homogenates of hamsters receiving study treatments after infection of SARS-CoV-2. PBS, phosphate buffer saline; COS, chitosan oligosaccharide; HCQ, hydroxychloroquine; Ct value, cycle threshold value.

Biochemistry data

Serum AST levels were significantly higher on day 8 in the COS group compared to all other groups (Fig. 2A). In the COS group, serum ALT levels were also significantly increased on days 4 and 8 (Fig. 2B). The COS + HCQ group exhibited significantly lower serum LDH levels on day 14 (Fig. 2C).

Serum IL-6 levels were significantly elevated in the COS + HCQ group on day 4 in comparison with all other groups (Fig. 3A). Similarly, the expression of IL-10 was significantly higher in the COS + HCQ group on day 8 (Fig. 3C). IgA levels on day 4 were significantly increased in the COS + HCQ, COS and HCQ groups (Fig. 3D), as were the IgG levels on day 14 (Fig. 3E). On day 8, IgA and IgG levels in the COS + HCQ group were significantly higher than all other groups (Fig. 3D and E).

Concentration of hydroxychloroquine

HCQ was detected only in the HCQ and COS + HCQ groups. HCQ concentrations in the lung tissue were numerically higher than that detected in the blood and bronchoalveolar lavage fluid in both groups. Notably, HCQ concentrations were higher in the lung tissue of the COS + HCQ group compared to hamsters that received HCQ only. This phenomenon was most pronounced on day 14 after infection.

Histopathology examination of the lungs, heart, and liver

In the PBS group, significant inflammation was evident on day 1, with the emergence of inflammatory cell aggregates and spotty hemorrhages on day 7. By day 14, necrosis and loss of normal alveolar structure were observed. Heavy mucus formation was notable since day 1 and worsened with time. IHC staining of the SARS-CoV-2 N protein showed prominent viral infiltration with diffuse persistence on day 14 (Fig. 4).

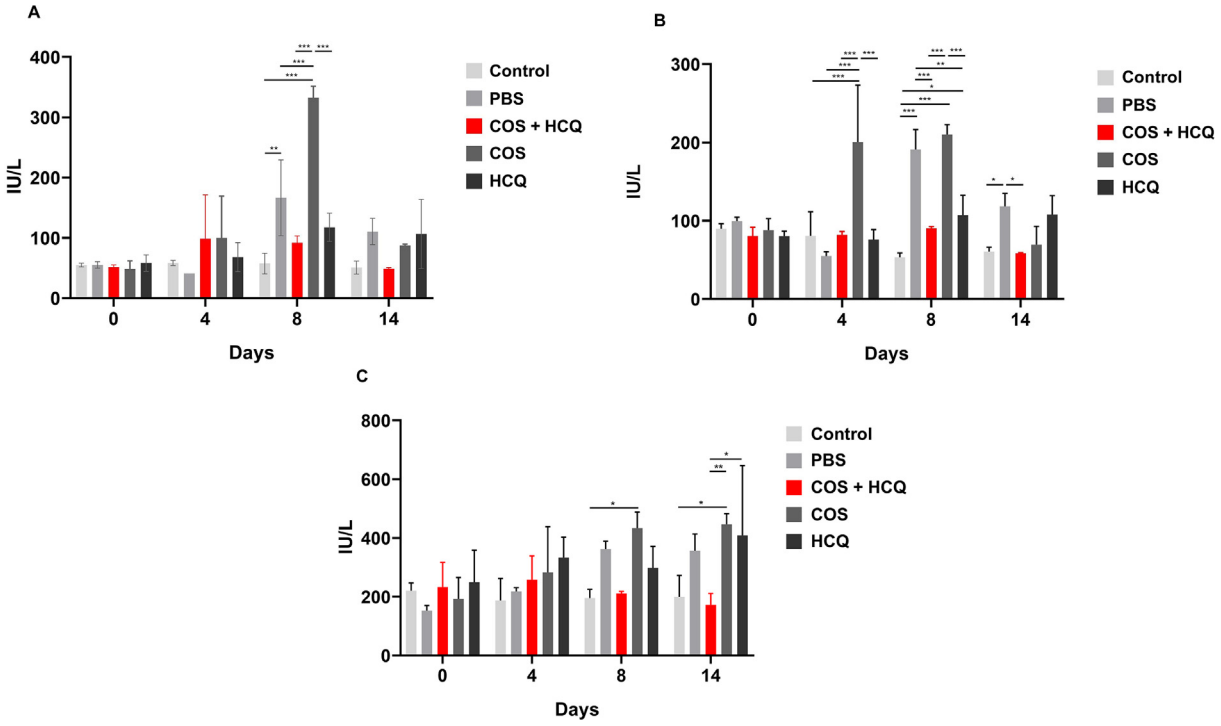

Figure 2. Serum AST (A), ALT (B), and LDH (C) levels in hamsters receiving study treatments after infection of SARS-CoV-2. AST, aspartate aminotransferase; ALT, alanine transaminase; LDH, lactate dehydrogenase; PBS, phosphate buffer saline; COS, chitosan oligosaccharide; HCQ, hydroxychloroquine.

H&E staining of the lungs from the COS group revealed significant perivascular inflammatory infiltrates with scattered hemorrhages throughout the parenchyma that persisted to day 14. Large amounts of mucin formation were noted by day 7, with obstruction of bronchial spaces observed on day 14. Viral protein stained densely on day 1 but regressed by day 14 (Fig. 5).

In the HCQ group, interstitial inflammation and spotty hemorrhages could be seen since day 1, with partial resolution of interstitial hemorrhages on day 14. PAS staining revealed markedly heavy mucus that filled the interstitium. Viral protein aggregates persisted throughout the study period, with slightly decreased staining in the parenchyma by day 14 (Fig. 6).

H&E stains of the COS + HCQ group on day 1 post-infection demonstrated inflammation that progressed in severity by day 7. However, inflammation and interstitial hemorrhages were almost entirely resolved by day 14. There is much less mucus seen in the COS + HCQ group compared to other groups throughout the entire period of observation. IHC staining demonstrated rapid clearance of viral infiltration, with decrease in staining already evident on day 7 (Fig. 7).

SEM examination of lung tissue slides was also performed. Pathology from the COS + HCQ group demonstrated intact pulmonary architectures, with the tissue clear of mucus formation or inflammatory cells (Supplemental Fig. 4). Pathology of the heart (Supplemental Fig. 5) and liver (Supplemental Fig. 6) from all groups did not reveal significant changes throughout days 1, 7 and 14.

Discussion

In this study, we assessed the efficacy and safety of a novel inhaled combination of COS + HCQ for treating COVID-19 in a hamster model. Our study revealed several findings. First, intranasal administration of combined COS + HCQ resulted in increased HCQ concentrations in the lung parenchyma compared to HCQ alone, suggesting that COS enhanced tissue penetration of drugs. Second, combined COS + HCQ led to earlier and greater immune responses, including acute production of IL-6 and IgA, and subsequent production of IL-10 and IgG. This was associated with faster viral clearance and attenuated lung injury. COS likely played immunomodulatory roles in this process. Third, intranasal administration of HCQ resulted in high local drug concentrations that was not associated with hepatic or cardiac injury. Inhalation of HCQ combined with COS is possibly a safe and efficacious means of treatment for COVID-19.

The SARS-CoV-2 virus infects its host by invading the respiratory epithelium[3]. HCQ inhibits SARS-CoV-2 infection through direct actions on the respiratory epithelial cell surface[19]. Because HCQ is extensively distributed in tissue, to achieve effective antiviral doses at the alveolar interface, large systemic doses are required.[20—22] Drug inhalation allows high local doses while limiting systemic side effects, whereas the site of drug deposition depends primarily on the size of inhaled particles. The optimal particle size for drug deposition in the lung is an aerodynamic diameter of approximately 0.5—5 μm[16]. The COS gel utilized in our study was dispersed into particles sized 0.3—10 μm, which allowed passage through the alveolar tissue barrier to other organs.

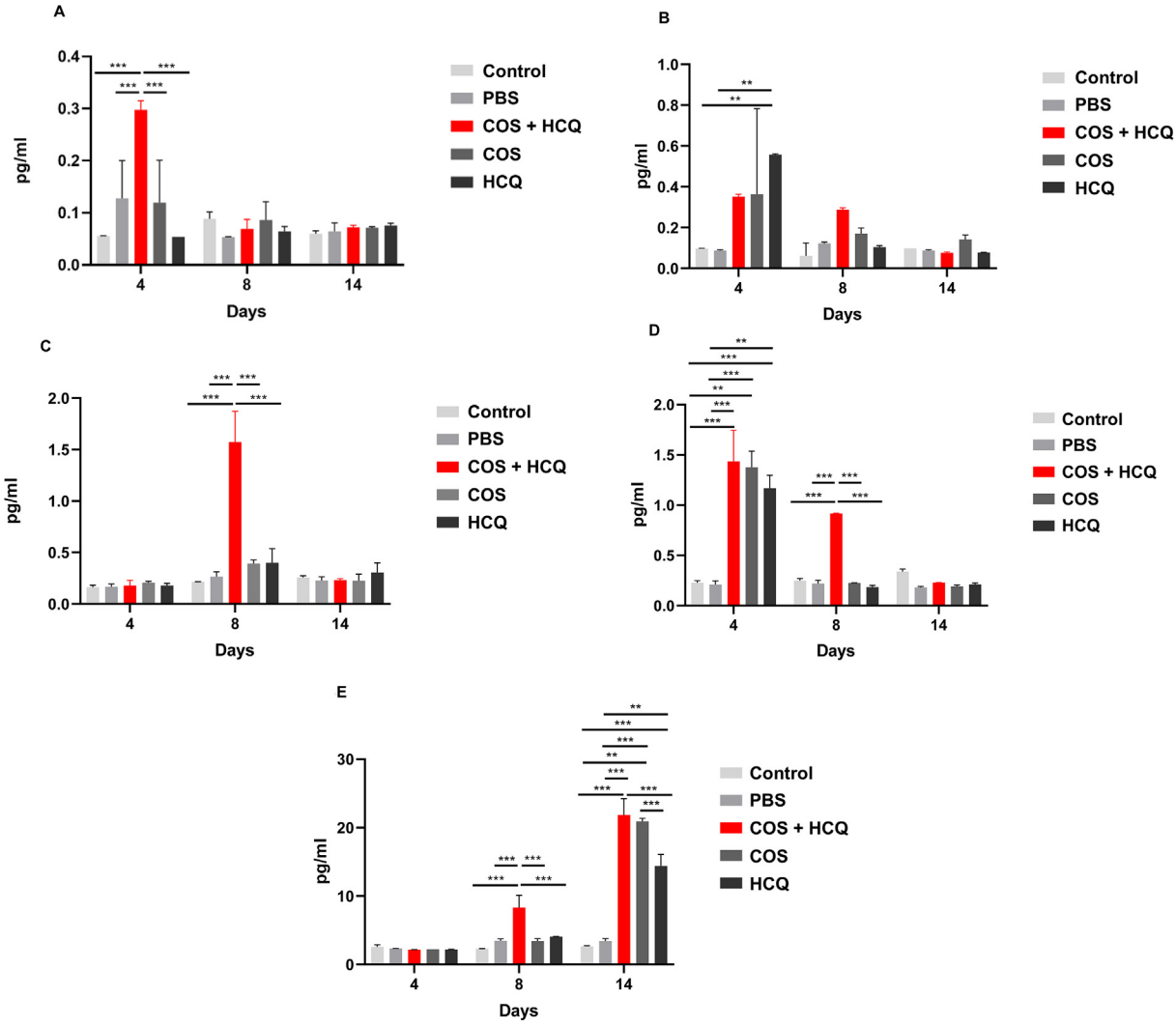

Figure 3. Serum IL-6 (A), IL-1β (B), IL-10 (C), IgA (D) and IgG (E) levels in hamsters receiving study treatments after infection of SARS-CoV-2. IL-6, interleukin-6; IL-1 β, interleukin-1 β; IL-10, interleukin-10; IgA, immunoglobulin A; IgG, immunoglobulin G; PBS, phosphate buffer saline; COS, chitosan oligosaccharide; HCQ, hydroxychloroquine.

Furthermore, chitosan molecules carry positive charges, leading to mucoadhesive properties and opening of intercellular tight junctions, enhancing drug absorption. We demonstrated that inhaled COS + HCQ was associated with increased HCQ concentration in the lung parenchyma compared to administration of HCQ only. Most importantly, this was achieved with half the inhaled dose of HCQ, further lowering the risk of systemic side effects and the costs of treatment. Furthermore, increased lung tissue HCQ concentrations were most evident on day 14, suggesting better retainment of the drug in the lungs with co-administration of COS. COS is likely a potent drug delivery vehicle that enhances lung absorption of HCQ.

Chitosan exhibits direct antiviral and immunomodulatory properties.[23] In this study, hamsters that received COS demonstrated earlier viral clearance on lung histopathology compared to PBS. In addition to antiviral effects, chitin and chitosan stimulate acute innate immune responses and promote subsequent humoral responses[23]. Chitin induces TH1 cell-mediated immunity and IL-10 production, leading to downregulation of pro-inflammatory cytokines.[24] Adding chitosan as an adjuvant to influenza vaccines also boosted immunogenicity in murine models.[25] The findings in our study conformed with those in literature. Hamsters treated with the combination of COS + HCQ expressed significantly higher levels of IL-6 on day 4 and IL-10 on day 8 after SARS-CoV-2 inoculation. The rapidity of IL-10 production suggests earlier activation of anti-inflammatory pathways that intervenes to prevent uncontrolled inflammation. IgA and IgG production were also greatly increased in this group. In particular, IgG levels were significantly higher in hamsters treated with COS + HCQ on day 8, suggesting earlier and more effective class switching of humoral responses.[26,27] These findings suggest that immune responses were more effective, better modulated, and greater in magnitude in hamsters treated with the COS + HCQ combination. Neither inhaled HCQ nor COS alone led to similar effects, indicating synergism between these two drugs.

The synergistic actions of COS and HCQ on the immune system may lead to earlier convalescence of disease with

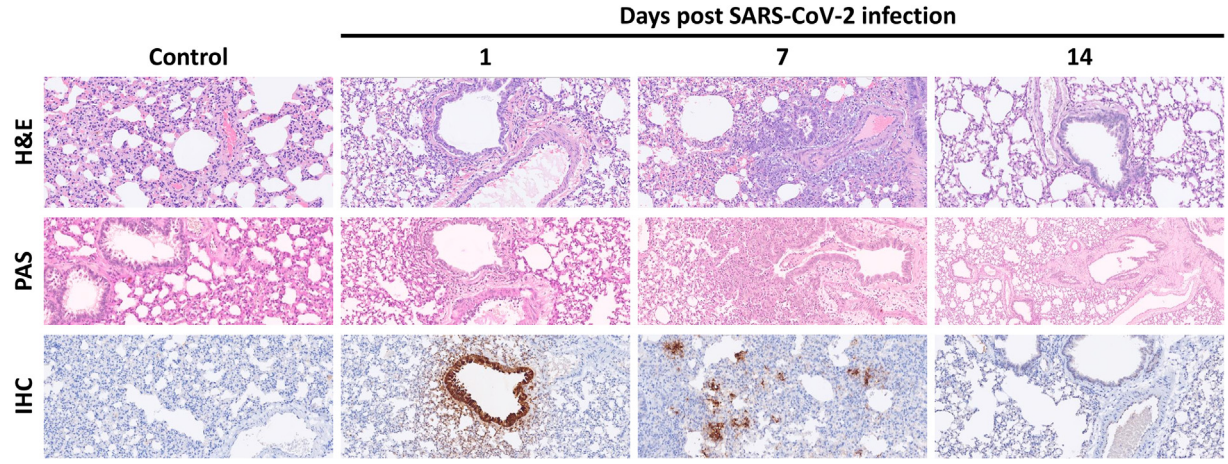

Figure 4. Histopathology of the lung in hamsters treated with PBS after SARS-CoV-2 infection. Significant peri-bronchiole and perivascular inflammatory cell infiltration was seen on day 1. By day 7, several foci of inflammatory cell aggregates were seen, accompanied by peri-bronchial and intra-alveolar hemorrhages. Inflammation persisted on day 14, with the necrosis and loss of lung tissue and cyst formation. Perivascular and peri-bronchial mucus formation was notable since day 1. Mucus was even more prominent on days 7 and 14, with progressive loss of lung tissue and cyst formation. IHC staining showed dense peri-bronchial staining on day 1, with subsequent spread to the lung parenchyma on day 7. There was diffuse persistent IHC reaction to SARS-CoV-2 N protein on day 14. H&E, hematoxylin and eosin stain; PAS, periodic-acid Schiff stain; IHC, immunohistochemistry; PBS, phosphate buffer saline.

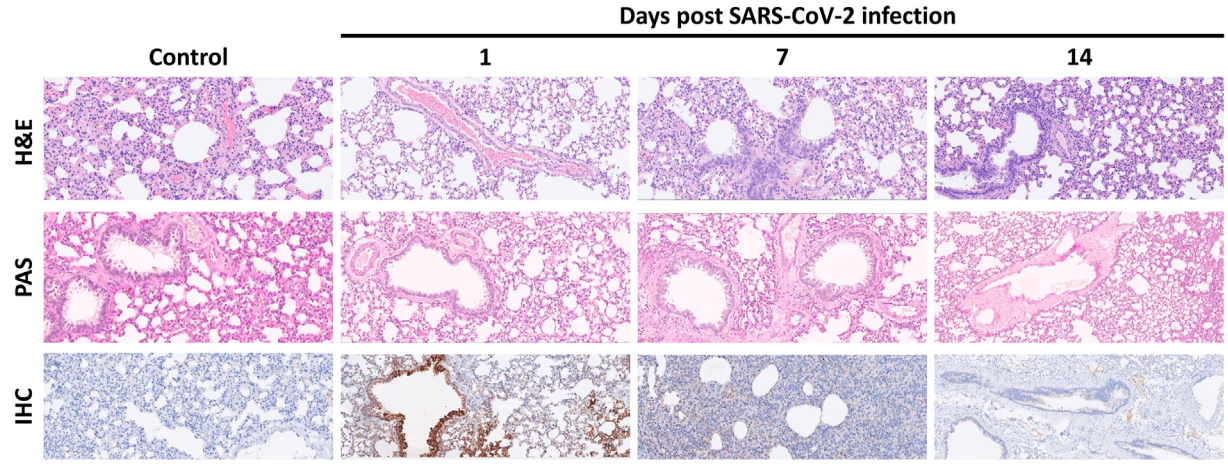

Figure 5. Histopathology of the lung in hamsters treated with COS after SARS-CoV-2 infection. Day 1 showed significant perivascular inflammatory infiltrates with scattered spots of hemorrhage throughout the parenchyma. On day 7, infiltration of inflammatory cells became for severe with diffuse parenchymal involvement and interstitial hemorrhage. Peri-bronchial inflammation and interstitial hemorrhage persisted in severity by day 14. Large amounts of mucin formation were noted in the interalveolar and perivascular interstitium on day 7. On day 14, heavy mucus production that filled bronchial spaces was still seen. IHC staining showed dense peri-bronchial staining with spreading to nearby tissue. Viral protein staining was more diffuse by day 7 but markedly regressed in density. By day 14, only minimal evidence of the presence of the SARS-CoV-2 N protein could be seen. H&E, hematoxylin and eosin stain; PAS, periodic-acid Schiff stain; IHC, immunohistochemistry; COS, chitosan oligosaccharide.

reduced organ injury. We found greater Ct values on day 8 in the COS + HCQ group, suggesting more rapid eradication of the virus. Histopathology of the lungs from the COS + HCQ group demonstrated earlier resolution of inflammation, limited production of mucus, and faster viral clearance. Although the COS + HCQ combination boosted immune defenses, the degree of inflammation was controlled, and adaptive immunity effectively induced. This suggests that the combination of COS + HCQ not only promotes earlier eradication of the SARS-CoV-2 but can also prevent the development of long-term post-COVID complications[6].

The greatest concerns regarding HCQ treatment for COVID-19 are systemic toxicities.[28] HCQ-associated cardiac and hepatic toxicities were more frequently reported among COVID-19 patients, as opposed to patients receiving HCQ for other conditions.[29] SARS-CoV-2 infection in itself can lead to acute liver injury, with transaminitis

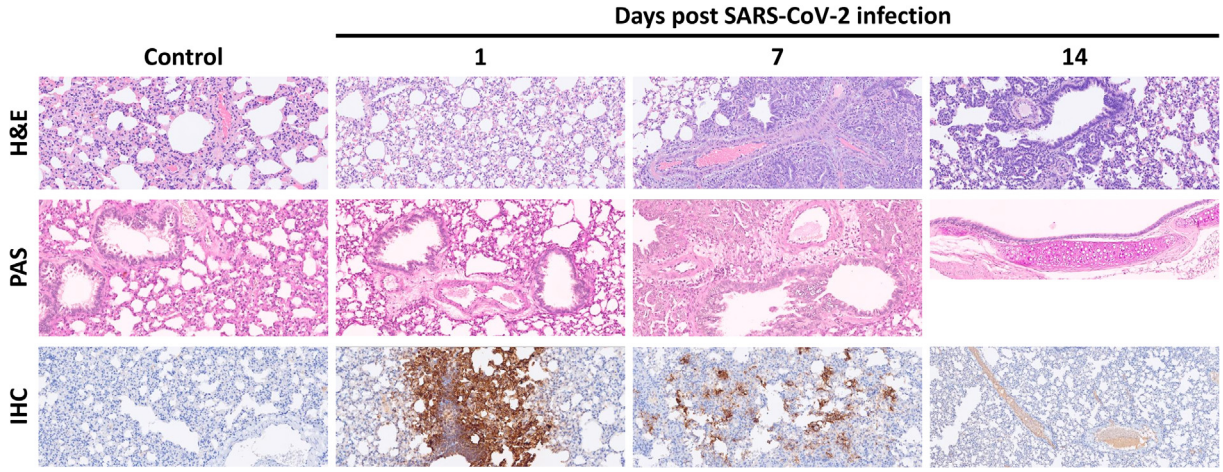

Figure 6. Histopathology of the lung in hamsters treated with HCQ after SARS-CoV-2 infection. Mild interstitial inflammation and spotty hemorrhages could be seen on day 1. Numerous foci of heavy inflammatory cell infiltration were observed on day 7, with a predominance of mononuclear cells. There was invasion of the capillary walls by inflammatory cells and intra-alveolar hemorrhage. By day 14, partial resolution of hemorrhage was evident, yet inflammation was more diffuse and severe. PAS staining showed mild mucin production on day 1, followed by the production of large amounts of mucus that filled the interstitium by day 7 and persisted to day 14. IHC staining showed large amounts of viral proteins in the bronchioles and with spread to the surrounding interstitium on day 1. On day 14, reduced staining for the viral protein was noted in the parenchyma, but significant reaction persisted in the capillaries and bronchioles. H&E, hematoxylin and eosin stain; PAS, periodic-acid Schiff stain; IHC, immunohistochemistry; HCQ, hydroxychloroquine.

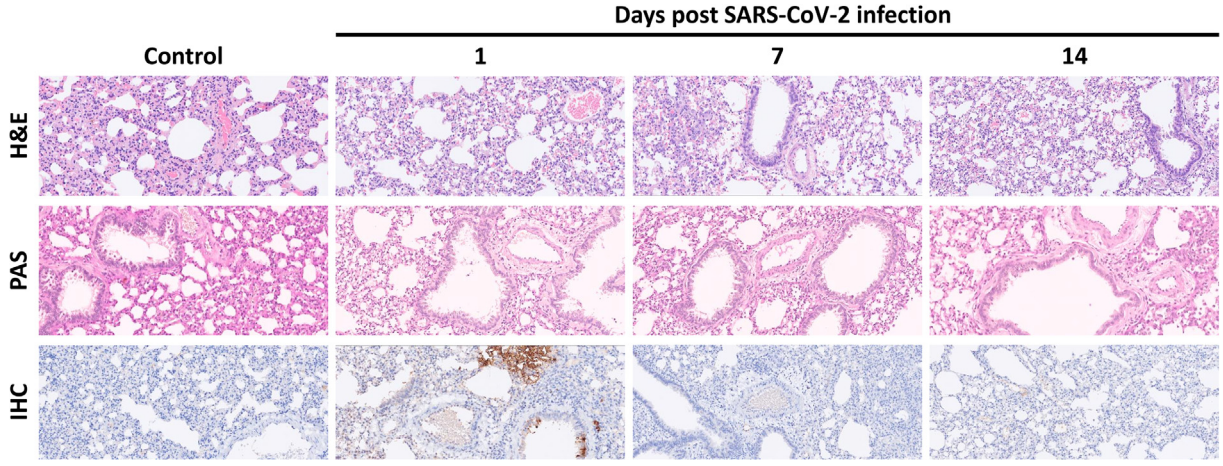

Figure 7. Histopathology of the lung in hamsters treated with COS + HCQ after SARS-CoV-2 infection. Generalized inflammation and interstitial hemorrhage could be seen on day 1 post-infection. Increased peri-bronchial inflammatory cell infiltrations with persistence of interstitial hemorrhages on day 7. The interstitial inflammatory cell infiltration was markedly decreased by day 14, with only minimal hemorrhage and inflammation evident under 20x magnification. There is little mucus production compared to other treatment groups, with complete resolution of mucus and alveolar structures remaining intact with PAS stain on day 14. IHC staining demonstrated marked decrease of viral proteins by day 7, and by day 14 the viral infiltrates have almost completely cleared. H&E, hematoxylin and eosin stain; PAS, periodic-acid Schiff stain; IHC, immunohistochemistry; COS, chitosan oligosaccharide; HCQ, hydroxychloroquine.

in the COVID-19 patient reflecting more severe disease.[30,31] In humans, drug-induced liver injury (DILI) often manifests with necro-inflammatory injury, cholestatic injury, and steatosis on histopathology.[32] COVID-related liver injury also present with steatosis, acute hepatitis, and portal inflammation[33–35]; thus, although COVID-19 patients are particularly vulnerable to drug-induced liver injury,[36] the differentiation between DILI and viral hepatitis is extremely difficult and requires consideration of the patient's blood tests, concomitant symptoms, and disease course as a whole. In our study, we assessed serum AST and ALT levels after virus inoculation and also examined hepatic pathology for signs of injury. Interestingly, hamsters exposed to HCQ had lower levels of serum AST and ALT compared to other groups. There was no evidence of hepatic injury on pathology examination.

Although it would be assertive to conclude that HCQ is protective against liver injury in hamsters with SARS-CoV-2 infection, our results suggest that HCQ, when administered via the respiratory tract at dosages sufficient to exert therapeutic effects locally, does not lead to hepatic toxicities.

This is a proof-of-concept study with several limitations. Our goal was to advocate inhaled COS as a novel adjuvant to inhaled HCQ in treating COVID-19. More data is needed to validate our findings. Although hamsters have been reportedly utilized as an animal model for COVID-19,[37,38] there is still relatively little experience in literature considering the recent emergence of this disease. Molecular reagents, such as antibodies, ELISA kits, and primers of PCR, may require more validation. Furthermore, in COVID-19 infections, the transition of viral invasion from the upper to lower respiratory tract is crucial in the development of severe disease. In our study, upper airway specimens were not examined due to limited resources laboratory constraints. Whether the inhaled combination of HCQ + COS may delay or impede this process is unknown from our results. Also, quantification of viral load by PCR or viral protein staining only cannot assess viral activity. Whether the virus is replicable from respiratory specimens or not may be crucial to demonstrate viral suppression. Lastly, the evaluation of HCQ-related liver and cardiac toxicities may not be entirely adequate by pathology alone. We present a proof-of-concept study with the goals of demonstrating safety, feasibility, and possible benefits of this therapy. Our results are hypothesis-generating and further investigations are necessary to translate our findings into clinical applications.

Conclusion

In hamsters infected with the SARS-CoV-2 virus, the combination of intranasal COS and HCQ was associated with increased HCQ absorption in the lungs, more rapid and effective immune responses, without increasing the risk of hepatic or cardiac injuries.

References

1. World Health Organization. *WHO Coronavirus (COVID-19) dashboard | WHO Coronavirus (COVID-19) dashboard with vaccination data [internet]. WHO Coronavirus (COVID-19) dashboard*. 2022 Aug 3. Available from: https://covid19.who.int/.
2. Caramaschi S, Kapp ME, Miller SE, Eisenberg R, Johnson J, Epperly G, et al. Histopathological findings and clinicopathologic correlation in COVID-19: a systematic review. *Mod Pathol* 2021 Sep;**34**(9):1614—33.
3. Osuchowski MF, Winkler MS, Skirecki T, Cajander S, Shankar-Hari M, Lachmann G, et al. The COVID-19 puzzle: deciphering pathophysiology and phenotypes of a new disease entity. *Lancet Respir Med* 2021 Jun;**9**(6):622—42.
4. Grasselli G, Zangrillo A, Zanella A, Antonelli M, Cabrini L, Castelli A, et al. Baseline characteristics and outcomes of 1591 patients infected with SARS-CoV-2 admitted to ICUs of the lombardy region. *Italy. JAMA*. 2020 Apr 28;**323**(16):1574—81.
5. Richardson S, Hirsch JS, Narasimhan M, Crawford JM, McGinn T, Davidson KW, et al. Presenting characteristics, comorbidities, and outcomes among 5700 patients hospitalized with COVID-19 in the New York city area. *JAMA* 2020 May 26;**323**(20):2052—9.
6. Lai C-C, Hsu C-K, Yen M-Y, Lee P-I, Ko W-C, Hsueh P-R. Long COVID: an inevitable sequela of SARS-CoV-2 infection. *J Microbiol Immunol Infect* 2022 Oct 15;**56**(1):1—9.
7. Pitre T, Van Alstine R, Chick G, Leung G, Mikhail D, Cusano E, et al. Antiviral drug treatment for nonsevere COVID-19: a systematic review and network meta-analysis. *CMAJ* 2022 Jul 25;**194**(28):E969—80.
8. Wang Y, Zhang D, Du G, Du R, Zhao J, Jin Y, et al. Remdesivir in adults with severe COVID-19: a randomised, double-blind, placebo-controlled, multicentre trial. *Lancet* 2020 May 16;**395**(10236):1569—78.
9. Jean S-S, Lee P-I, Hsueh P-R. Treatment options for COVID-19: the reality and challenges. *J Microbiol Immunol Infect* 2020 Jun;**53**(3):436—43.
10. Liu J, Cao R, Xu M, Wang X, Zhang H, Hu H, et al. Hydroxychloroquine, a less toxic derivative of chloroquine, is effective in inhibiting SARS-CoV-2 infection in vitro. *Cell Discov* 2020;**6**:16.
11. Yendrapalli U, Ali H, Green JL, Edwards J. Effects of cardiac toxicity of combination therapy with hydroxychloroquine and azithromycin in COVID-19 patients. *J Infect Public Health* 2021 Nov;**14**(11):1668—70.
12. Gumilang RA, Siswanto, Anggraeni VY, Trisnawati I, Budiono E, Hartopo AB. QT interval and repolarization dispersion changes during the administration of hydroxychloroquine/chloroquine with/without azithromycin in early COVID 19 pandemic: a prospective observational study from two academic hospitals in Indonesia. *J Arrhythm* 2021 Oct;**37**(5):1184—95.
13. Boulware DR, Pullen MF, Bangdiwala AS, Pastick KA, Lofgren SM, Okafor EC, et al. A randomized trial of hydroxychloroquine as postexposure prophylaxis for covid-19. *N Engl J Med* 2020 Aug 6;**383**(6):517—25.
14. Rosenberg ES, Dufort EM, Udo T, Wilberschied LA, Kumar J, Tesoriero J, et al. Association of treatment with hydroxychloroquine or azithromycin with in-hospital mortality in patients with COVID-19 in New York state. *JAMA* 2020 Jun 23;**323**(24):2493—502.
15. Magagnoli J, Narendran S, Pereira F, Cummings TH, Hardin JW, Sutton SS, et al. Outcomes of hydroxychloroquine usage in United States veterans hospitalized with COVID-19. *Med (N Y)* 2020 Dec 18;**1**(1):114—127.e3.
16. Borghardt JM, Kloft C, Sharma A. Inhaled therapy in respiratory disease: the complex interplay of pulmonary kinetic processes. *Cancer Res J* 2018 Jun 19;**2018**:2732017.
17. Mitchell JP, Berlinski A, Canisius S, Cipolla D, Dolovich MB, Gonda I, et al. Urgent appeal from international society for aerosols in medicine (ISAM) during COVID-19: clinical Decision makers and governmental agencies should consider the inhaled route of administration: a statement from the ISAM regulatory and standardization issues networking group. *J Aerosol Med Pulm Drug Deliv* 2020 Aug;**33**(4):235—8.
18. Shim S, Yoo HS. The application of mucoadhesive chitosan nanoparticles in nasal drug delivery. *Mar Drugs* 2020 Nov 29;**18**(12).
19. Yuan Z, Pavel MA, Wang H, Kwachukwu JC, Mediouni S, Jablonski JA, et al. Hydroxychloroquine blocks SARS-CoV-2 entry into the endocytic pathway in mammalian cell culture. *Commun Biol* 2022 Sep 14;**5**(1):958.
20. McChesney EW, Banks WF, Fabian RJ. Tissue distribution of chloroquine, hydroxychloroquine, and desethylchloroquine in the rat. *Toxicol Appl Pharmacol* 1967 May;**10**(3):501—13.
21. Browning DJ. *Pharmacology of chloroquine and hydroxychloroquine. Hydroxychloroquine and chloroquine retinopathy*. New York, NY: Springer New York; 2014. p. 35—63.
22. Ducharme J, Farinotti R. Clinical pharmacokinetics and metabolism of chloroquine. Focus on recent advancements. *Clin Pharmacokinet* 1996 Oct;**31**(4):257—74.

23. Safarzadeh M, Sadeghi S, Azizi M, Rastegari-Pouyani M, Pouriran R, Haji Molla Hoseini M. Chitin and chitosan as tools to combat COVID-19: a triple approach. *Int J Biol Macromol* 2021 Jul 31;**183**:235—44.
24. Lee CG, Da Silva CA, Lee J-Y, Hartl D, Elias JA. Chitin regulation of immune responses: an old molecule with new roles. *Curr Opin Immunol* 2008 Dec;**20**(6):684—9.
25. Ghendon Y, Markushin S, Krivtsov G, Akopova I. Chitosan as an adjuvant for parenterally administered inactivated influenza vaccines. *Arch Virol* 2008 Feb 23;**153**(5):831—7.
26. Li C-H, Chiou H-YC, Lin M-H, Kuo C-H, Lin Y-C, Lin Y-C, et al. Immunological map in COVID-19. *J Microbiol Immunol Infect* 2021 Aug;**54**(4):547—56.
27. Lin Y-C, Lee Y-L, Cheng C-Y, Tseng W-P, Wu J-L, Lin C-H, et al. Multicenter evaluation of four immunoassays for the performance of early diagnosis of COVID-19 and assessment of antibody responses of patients with pneumonia in Taiwan. *J Microbiol Immunol Infect* 2021 Oct;**54**(5):816—29.
28. Singh B, Ryan H, Kredo T, Chaplin M, Fletcher T. Chloroquine or hydroxychloroquine for prevention and treatment of COVID-19. *Cochrane Database Syst Rev* 2021 Feb 12;**2**(2):CD013587.
29. Sainz-Gil M, Merino Kolly N, Velasco-González V, Verde Rello Z, Fernandez-Araque AM, Sanz Fadrique R, et al. Hydroxychloroquine safety in Covid-19 vs non-Covid-19 patients: analysis of differences and potential interactions. *Expet Opin Drug Saf* 2022 May 19:1—9.
30. Cavuşoğlu Türker B, Türker F, Ahbab S, Hoca E, Urvasızoğlu AO, Cetin SI, et al. Evaluation of the charlson comorbidity index and laboratory parameters as independent early mortality predictors in covid 19 patients. *Int J Gen Med* 2022 Jul 27;**15**:6301—7.
31. Shaveisi-Zadeh F, Nikkho B, Khadem Erfan MB, Amiri A, Azizi A, Mansouri N, et al. Changes in liver enzymes and association with prognosis in patients with COVID-19: a retrospective case-control study. *J Int Med Res* 2022;**50**(7):3000605221110067.
32. European Association for the Study of the Liver. Electronic address: easloffice@easloffice.eu, clinical practice guideline panel: chair:, panel members, EASL governing board representative: EASL clinical practice guidelines: drug-induced liver injury. *J Hepatol* 2019 Jun;**70**(6):1222—61.
33. Lagana SM, Kudose S, Iuga AC, Lee MJ, Fazlollahi L, Remotti HE, et al. Hepatic pathology in patients dying of COVID-19: a series of 40 cases including clinical, histologic, and virologic data. *Mod Pathol* 2020 Nov;**33**(11):2147—55.
34. Zhao CL, Rapkiewicz A, Maghsoodi-Deerwester M, Gupta M, Cao W, Palaia T, et al. Pathological findings in the postmortem liver of patients with coronavirus disease 2019 (COVID-19). *Hum Pathol* 2021 Mar;**109**:59—68.
35. Sonzogni A, Previtali G, Seghezzi M, Grazia Alessio M, Gianatti A, Licini L, et al. Liver histopathology in severe COVID 19 respiratory failure is suggestive of vascular alterations. *Liver Int* 2020 Sep;**40**(9):2110—6.
36. Sodeifian F, Seyedalhosseini ZS, Kian N, Eftekhari M, Najari S, Mirsaeidi M, et al. Drug-induced liver injury in COVID-19 patients: a systematic review. *Front Med (Lausanne)* 2021 Sep 20;**8**:731436.
37. Bednash JS, Kagan VE, Englert JA, Farkas D, Tyurina YY, Tyurin VA, et al. Syrian hamsters as a model of lung injury with SARS-CoV-2 infection: pathologic, physiologic, and detailed molecular profiling. *Transl Res* 2022 Feb;**240**:1—16.
38. Yang S-J, Wei T-C, Hsu C-H, Ho S-N, Lai C-Y, Huang S-F, et al. Characterization of virus replication, pathogenesis, and cytokine responses in Syrian hamsters inoculated with SARS-CoV-2. *J Inflamm Res* 2021 Aug 11;**14**:3781—95.

Appendix A. Supplementary data

Supplementary data to this article can be found online at https://doi.org/10.1016/j.jmii.2023.08.001.